NeuroImage: Clinical 21 (2019) 101630

Contents lists available at ScienceDirect

NeuroImage: Clinical

journal homepage: www.elsevier.com/locate/ynicl

Characterisation of brain volume and microstructure at term-equivalent age in infants born across the gestational age spectrum

Deanne K. Thompson[a,b,c,*], Claire E. Kelly[a], Jian Chen[a,d], Richard Beare[a,d], Bonnie Alexander[a], Marc L. Seal[a,c], Katherine J. Lee[a,c], Lillian G. Matthews[a,c,e], Peter J. Anderson[a,c,f], Lex W. Doyle[a,c,g,h], Jeanie L.Y. Cheong[a,g,h], Alicia J. Spittle[a,g,i]

[a] Murdoch Children's Research Institute, Melbourne, VIC, Australia
[b] Florey Institute of Neuroscience and Mental Health, Melbourne, VIC, Australia
[c] Department of Paediatrics, The University of Melbourne, Melbourne, VIC, Australia
[d] Department of Medicine, Monash University, Melbourne, Australia
[e] Department of Newborn Medicine, Harvard Medical School, Brigham and Women's Hospital, Boston, MA, USA
[f] Monash Institute of Cognitive and Clinical Neurosciences, Monash University, Melbourne, VIC, Australia
[g] Neonatal Services, The Royal Women's Hospital, Melbourne, VIC, Australia
[h] Department of Obstetrics and Gynaecology, The University of Melbourne, Melbourne, VIC, Australia
[i] Department of Physiotherapy, The University of Melbourne, Melbourne, VIC, Australia

ARTICLE INFO

Keywords:
Magnetic resonance imaging
Diffusion weighted imaging
Preterm
Premature birth
Neonate

ABSTRACT

Background: Risk of morbidity differs between very preterm (VP; < 32 weeks' gestational age (GA)), moderate preterm (MP; 32–33 weeks' GA), late preterm (LP; 34–36 weeks' GA), and full-term (FT; ≥37 weeks' GA) infants. However, brain structure at term-equivalent age (TEA; 38–44 weeks) remains to be characterised in all clinically important GA groups. We aimed to compare global and regional brain volumes, and regional white matter microstructure, between VP, MP, LP and FT groups at TEA, in order to establish the magnitude and anatomical locations of between-group differences.

Methods: Structural images from 328 infants (91 VP, 63 MP, 104 LP and 70 FT) were segmented into white matter, cortical grey matter, cerebrospinal fluid (CSF), subcortical grey matter, brainstem and cerebellum. Global tissue volumes were analysed, and additionally, cortical grey matter and white matter volumes were analysed at the regional level using voxel-based morphometry. Fractional anisotropy (FA), mean diffusivity (MD), axial diffusivity (AD) and radial diffusivity (RD) images from 361 infants (92 VP, 69 MP, 120 LP and 80 FT) were analysed using Tract-Based Spatial Statistics. Statistical analyses involved examining the overall effect of GA group on global volumes (using linear regressions) and regional volumes and microstructure (using non-parametric permutation testing), as well performing post-hoc comparisons between the GA sub-groups.

Results: On global analysis, cerebrospinal fluid (CSF) volume was larger in all preterm sub-groups compared with the FT group. On regional analysis, volume was smaller in parts of the temporal cortical grey matter, and parts of the temporal white matter and corpus callosum, in all preterm sub-groups compared with the FT group. FA was lower, and RD and MD were higher in voxels located in much of the white matter in all preterm sub-groups compared with the FT group. The anatomical locations of group differences were similar for each preterm vs. FT comparison, but the magnitude and spatial extent of group differences was largest for the VP, followed by the MP, and then the LP comparison. Comparing within the preterm groups, the VP sub-group had smaller frontal and temporal grey and white matter volume, and lower FA and higher MD and RD within voxels in the approximate location of the corpus callosum compared with the MP sub-group. There were few volume and microstructural differences between the MP and LP sub-groups.

Conclusion: All preterm sub-groups had atypical brain volume and microstructure at TEA when compared with a

Abbreviations: AD, axial diffusivity; ANOVA, analysis of variance; BET, brain extraction tool; CI, confidence interval; FA, fractional anisotropy; FOV, field of view; FSL, Functional magnetic resonance imaging of the brain Software Library; FT, full-term; FUGUE, Functional magnetic resonance imaging of the brain's Utility for Geometrically Unwarping Echo planar images; GA, gestational age; LP, late preterm; MANTiS, morphologically adaptive neonatal tissue segmentation; MD, mean diffusivity; MP, moderate preterm; MRI, magnetic resonance imaging; RD, radial diffusivity; SPM, statistical parametric mapping; TBSS, tract-based spatial statistics; TE, echo time; TEA, term-equivalent age; TR, repetition time; VBM, voxel based morphometry; VP, very preterm

* Corresponding author.
E-mail address: deanne.thompson@mcri.edu.au (D.K. Thompson).

https://doi.org/10.1016/j.nicl.2018.101630
Received 6 July 2018; Received in revised form 3 December 2018; Accepted 7 December 2018
Available online 10 December 2018

FT group, particularly for the CSF, temporal grey and white matter, and corpus callosum. In general, the groups followed a gradient, where the differences were most pronounced for the VP group, less pronounced for the MP group, and least pronounced for the LP group. The VP sub-group was particularly vulnerable compared with the MP and LP sub-groups.

1. Introduction

The rate of preterm birth (defined as < 37 weeks' gestational age (GA)) is rising worldwide, and preterm birth is a leading cause of infant mortality, morbidity and developmental impairments (Blencowe et al., 2013). Preterm birth is commonly sub-categorised into extremely preterm (< 28 weeks), very preterm (VP; < 32 weeks), moderate preterm (MP; 32–34 weeks), and late preterm (LP; 34–36 weeks) birth (Engle, 2006; Raju et al., 2006; Shapiro-Mendoza and Lackritz, 2012). These GA groups are known to have different clinical risk profiles (Thompson et al., 2019). Rates of perinatal morbidities and neurodevelopmental impairments in childhood are highest in extremely preterm and VP groups, lower in MP groups, and lower again in LP groups, but still higher in MP and LP groups compared with groups of infants born full-term (FT) (Altman et al., 2011; Ancel et al., 2015; Cheong et al., 2017; Lindstrom et al., 2007; Manuck et al., 2016; Moster et al., 2008; Teune et al., 2011; Yaari et al., 2018).

Brain structure at term-equivalent age (TEA; 38–44 weeks' post-menstrual age) has been thoroughly documented for those born earliest, where research studies often group together the extremely preterm with the VP infants, hence these groups were also combined in the current manuscript. Magnetic resonance imaging (MRI) studies have shown that VP infants have smaller cortical and subcortical grey matter and myelinated white matter volumes compared with FT infants (Inder et al., 2005). Other regional brain volumes (Thompson et al., 2007), including the basal ganglia and thalamus (Boardman et al., 2006), cerebellum (Shah et al., 2006), and hippocampus (Thompson et al., 2008) are also smaller in VP infants compared with FT infants. Diffusion MRI studies have shown that VP infants have microstructural alterations throughout much of the white matter compared with FT infants at TEA (Thompson et al., 2014), particularly in the posterior limb of the internal capsule, centrum semiovale, corpus callosum, corona radiata and central and frontal white matter (Alexandrou et al., 2014; Anjari et al., 2007; Huppi et al., 1998; Pogribna et al., 2013). Despite these many studies on VP infants, there have been few studies of the wider preterm spectrum, including VP, MP and LP infants. We have recruited and obtained MRI data for a large cohort of infants born across the GA spectrum, which uniquely enables us to examine brain volumes and microstructure in VP, MP, LP and FT groups (Spittle et al., 2014; Walsh et al., 2014). We have previously used this cohort to investigate white matter microstructure in the combined MP and LP groups in relation to FT infants (Kelly et al., 2016). We also recently investigated the relationships of specific perinatal medical and socio-demographic factors (birth weight, sex, multiple birth, and social risk) with brain volumes and microstructure (Thompson et al., 2019). However, to date brain structure, including volume and microstructure, has not been compared between all the clinically important GA groups, namely MP and LP groups in relation to VP and FT groups. This means the possible GA gradient of brain structure in infants born across the GA spectrum has not been studied.

We have recently developed the Morphologically Adaptive Neonatal Tissue Segmentation (MANTiS) technique for automatically segmenting neonatal brain images, including images with abnormalities common in preterm infants, into cortical grey matter, white matter, cerebrospinal fluid, subcortical grey matter, cerebellum, and brainstem (Beare et al., 2016). MANTiS generates segmentations in native space and in the standard space of a neonatal template (Kuklisova-Murgasova et al., 2011), and therefore facilitates analysis of global brain volumes and regional (voxel-wise) volumes using voxel-based morphometry (VBM). Analysing brain volumes both at the global level and regional level is important, to identify possible global effects on the preterm brain, and brain regions of heightened vulnerability that might provide greater understanding of functional impairments in specific motor, cognitive or behavioural domains (Cheong et al., 2017). Brain white matter microstructure can be analysed using diffusion MRI analysis techniques such as Tract-Based Spatial Statistics (TBSS), a commonly adopted technique that enables a global, voxel-wise survey of white matter microstructure (Smith et al., 2006).

The overall goal of this study was to characterise brain structure at TEA in the clinically important GA groups. Specifically, we aimed to: (1) compare global and regional brain volumes, and regional white matter microstructure, between each of the preterm sub-groups (VP, MP, LP) and the FT group at TEA, in order to establish the magnitudes and anatomical locations of any between-group differences; and (2) to compare the preterm sub-groups to each other, to determine whether particular preterm sub-groups have specific brain vulnerabilities at TEA. In line with the clinical risks of the GA groups, we expected that brain structure in the GA groups would follow a gradient, whereby brain alterations would be more pronounced in the earlier-born GA groups.

2. Methods

2.1. Recruitment

551 infants were recruited into different prospective cohort studies from the Royal Women's Hospital, Melbourne between November 2009 and May 2014. These included 149 VP (< 30 weeks' GA), 73 MP and 128 LP infants without congenital abnormalities likely to affect brain growth or development, as well as 201 healthy FT infants. The selection criteria for each of the cohorts did not include infants born at 30 or 31 weeks' GA. The cohorts have been previously described (Spittle et al., 2014; Walsh et al., 2014). Ethical approval for the studies was obtained from the Human Research Ethics Committees of the Royal Women's Hospital and the Royal Children's Hospital, Melbourne (where MRI was conducted). Written informed consent was obtained from all parents.

2.2. Magnetic resonance imaging

MRI was performed at the Royal Children's Hospital, Melbourne on a 3 T Siemens Magnetom Trio, Tim system at TEA. Infants were fed, swaddled, placed in a MedVac bag (CFI Medical Solutions Inc., Fenton, Michigan), and scanned while sleeping, without sedation or anaesthesia using the same imaging protocol for all infants. T_2-weighted turbo spin echo images were acquired in around 5 min with the following parameters: repetition time (TR) 8910 ms, echo time (TE) 152 ms, flip angle 120°, field of view (FOV) 192 × 192 mm, matrix 192 × 192, 99 axial slices, 1 mm^3 isotropic voxels. Diffusion-weighted images were acquired in around 19 min using a multi-*b*-value, echo planar imaging (EPI) sequence with the following parameters: TR 20400 ms, TE 120 ms, FOV 173 × 173 mm, matrix 144 × 144, 100 axial slices, 1.2 mm^3 isotropic voxels, 45 non-collinear gradient directions, *b*-values ranging from 100 to 1200 s/mm^2 in increments of 50 (23 different *b*-values in total, with 1–3 gradient directions per *b*-value), three $b = 0$ s/mm^2 volumes. The total diffusion sequence (45 directions plus three $b = 0$ s/mm^2 volumes) was divided into three separate acquisitions (17 directions requiring ≈6 min, 16 directions requiring ≈5 min 40 s, and 15 directions

requiring ≈5 min 30 s) to improve compliance, and if any of the diffusion acquisitions had unacceptable levels of motion artifact, the scan was repeated whenever possible until acceptable diffusion images were acquired. All infants were scanned with the same diffusion sequence, including the same range of *b*-values. This diffusion sequence was, at the time of recruitment, an advanced acquisition scheme optimised for the neonatal and preterm brain, with the range of *b*-values chosen to allow better characterisation of the biophysical properties of water diffusion in tissues and enable more sophisticated diffusion modeling. Of the eligible infants included in this study, 397 infants were scanned, but 9 were subsequently excluded as they were scanned > 44 weeks' GA. The main reason infants were not scanned was parental preference, considering MRI was an optional part of the studies. Further exclusions due to incomplete MRI, movement or other imaging artifact affecting data quality meant that a total of 328 infants were included in the volumetric analyses, and 361 in the diffusion analyses (Fig. 1). For the diffusion analyses, individual infants were excluded entirely if excessive movement was present within their diffusion sequence (14 infants were excluded for this reason), rather than removing individual diffusion volumes. Given our multiple *b*-value sequence, removal of individual volumes may introduce bias due to inhomogeneous gradient directions between groups. Thus, all included infants had the same number of diffusion volumes.

2.3. T_2-weighted image processing

T_2 images were bias corrected (Tustison et al., 2010) in order to improve skull-stripping using the Brain Extraction Tool (BET) from the Oxford Centre for Functional MRI of the Brain (FMRIB) Software Library (FSL) (Smith, 2002), and segmented into white matter, cortical grey matter, cerebrospinal fluid, subcortical grey matter (including deep nuclear grey matter, hippocampus and amygdala), brainstem, and cerebellum using the MANTiS technique (Beare et al., 2016). MANTiS is an extension of unified segmentation in Statistical Parametric Mapping (SPM) software, but it has modifications for neonatal images, including the use of a neonatal template, as detailed previously (Beare et al., 2016). MANTiS generates brain tissue volumes in native space and segmentation maps in the standard space of the Imperial College London neonatal template (Kuklisova-Murgasova et al., 2011). Each participant's registration to the neonatal template was visually examined, and one infant was excluded due to having poor registration. Standard-space maps for cortical grey matter and white matter were combined into 4D files, which were smoothed with a full-width half-maximum kernel of 2 mm and analysed using VBM in SPM software (Ashburner and Friston, 2000).

2.4. Diffusion-weighted image processing

Diffusion images were corrected for head motion and eddy current induced distortions using FSL's eddy-correct (Jenkinson and Smith, 2001), incorporating *b*-vector reorientation (Leemans and Jones, 2009). We also calculated motion parameters (absolute and relative displacement, translation and rotation) and compared them between the GA groups. There was little evidence for differences in the motion parameters between groups, suggesting that motion is not responsible for our reported differences in diffusion tensor measures between the GA groups. Echo planar image distortions due to magnetic field inhomogeneity were corrected based on a gradient echo field map. The field map image that we used was the average of a subset of $n = 10$ participants' field map images ($n = 8$ preterm and $n = 2$ FT). We used an average field map from 10 participants because field maps were not acquired for all participants. The field inhomogeneity due to the scanner was assumed to be stable across participants. The average field map was non-linearly registered to the *b*0 image of each participant. Distortions were then corrected using the aligned field map and FMRIB's Utility for Geometrically Unwarping Echo planar images (FUGUE). The diffusion tensor model was fitted to diffusion images using the weighted linear least squares method in FSL, appropriate for this multi *b*-value sequence (Veraart et al., 2013), generating fractional anisotropy (FA), mean diffusivity (MD), axial diffusivity (AD) and radial diffusivity (RD) images. FSL's TBSS (Smith et al., 2006) was used to analyse the diffusion tensor data. All possible pairwise registrations between infants' FA images were performed using FSL's non-linear registration tool. This was conducted to identify the most representative infant's FA image (i.e. the study specific target image), which was chosen as the infant's FA image that had the minimum mean displacement required to align it to all the other infants' FA images. All FA images were then aligned to the study specific target image, following

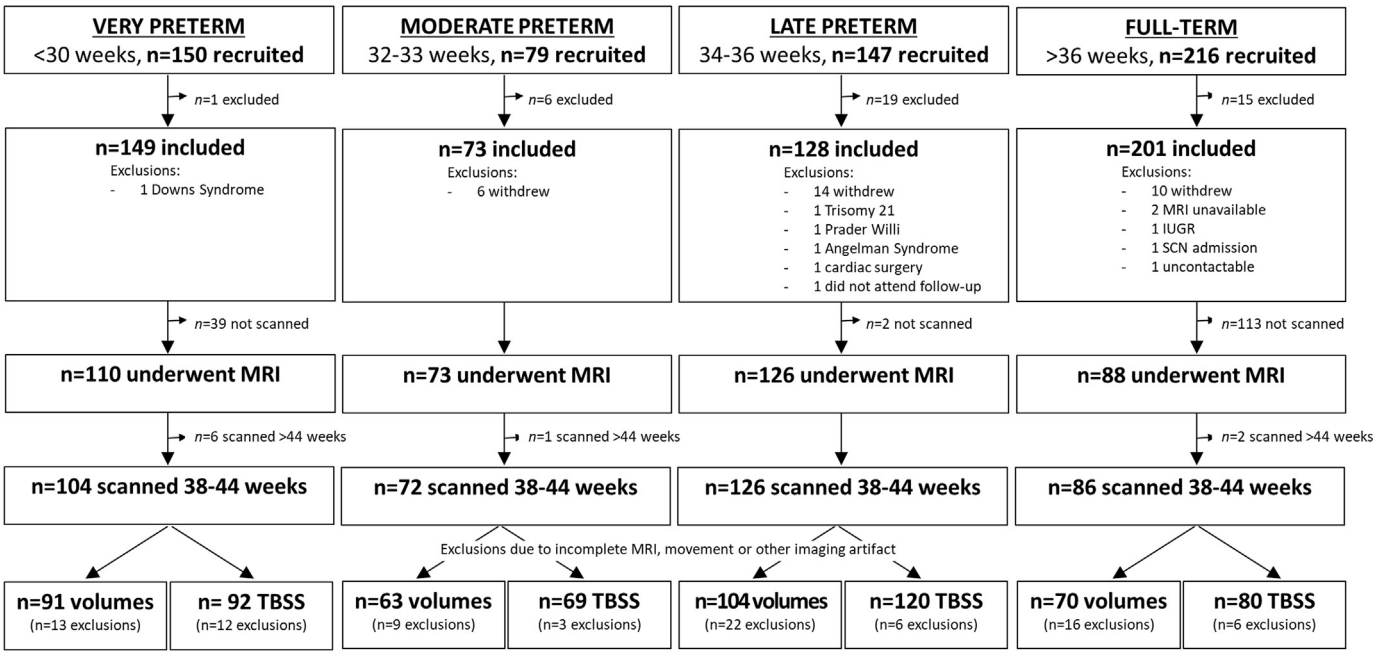

Fig. 1. Recruitment and inclusions flowchart for study participants.
MRI = magnetic resonance imaging; IUGR = intrauterine growth restriction; SCN = special care nursery; TBSS = tract-based spatial statistics.

the general recommendations documented by FSL for studies involving young children. The resulting transformation matrix was nonlinearly applied to the MD, AD and RD images. A mean FA image was created and thinned to generate a mean FA skeleton, thresholded at 0.2. We visually inspected the mean FA skeleton and found that it included all major white matter tracts, whilst mostly excluding other tissue types (grey matter or cerebrospinal fluid). The aligned MD, AD and RD images were also projected onto the mean FA skeleton.

2.5. Statistical analyses

Participant characteristics were compared between infants who had useable MRI data and the remaining infants who were recruited but could not be included in the current study using *t*-tests, Mann-Whitney *U* tests, or $\chi 2$ tests as appropriate.

Stata 14.1 was used for global brain volume analyses. Separate linear regressions were used to determine the overall effect of GA group on brain volumes (total intracranial, brain tissue, white matter, cortical grey matter, subcortical grey matter, cerebrospinal fluid, cerebellum, and brainstem volumes). Models were fitted using generalised estimating equations to allow for clustering for multiple births and were adjusted for postmenstrual age at MRI. The FT group was used as the reference group. Post-hoc tests were used to determine whether there were any group-wise differences between each preterm sub-group and the FT group, and between preterm sub-groups. Each analysis was false discovery rate-corrected for the number of brain volumes (8).

To explore the effect of GA group on regional (voxel-wise) brain cortical grey matter and white matter volume (derived from VBM) and white matter microstructure (derived from TBSS), non-parametric permutation-based testing was performed using FSL's Randomise. Firstly, a statistical design file was created using FSL's 'General Linear Model (Glm)' tool. A '1-factor 4-levels analysis of variance (ANOVA)' model was constructed. This Glm design had one F-test for the overall effect of GA group (VP, MP, LP or FT) on voxel-wise volumes (cortical grey matter, white matter) and diffusion parameters (FA, AD, RD, MD), and 12 contrasts for the individual comparisons of voxel-wise volumes and diffusion parameters between all of the GA groups. In all tests, postmenstrual age at MRI was included as a covariate. Results were not adjusted for intracranial volume because the aim of the study was to compare brain volumes of specific regions between GA groups and not to determine which brain regions were most vulnerable over and above total intracranial volume differences. Results are reported at the $p < .05$ level after 5000 permutations, threshold-free cluster enhancement and family-wise error rate correction for multiple comparisons. Regions of statistical significance were localised to anatomical regions by linearly registering a neonatal template and atlas (Oishi et al., 2011) to our T_2 template (for VBM) or to our mean FA image (for TBSS) using FSL. We also linearly registered our mean FA image to our T_2 template and applied this registration to the masks of the significant TBSS regions, to calculate the overlap between the TBSS and VBM significant regions, using FSL.

3. Results

3.1. Participant characteristics

Ninety-one VP, 63 MP, 104 LP ($n = 103$ for VBM analysis due to suboptimal alignment in one subject) and 70 FT infants had tissue segmentations of sufficient quality to be included for volumetric analyses, and 92 VP, 69 MP, 120 LP and 80 FT infants had diffusion data of sufficient quality for inclusion in TBSS analyses (Table 1).

Perinatal characteristics of the VP, MP, LP and FT infants are shown

Table 1
Participant characteristics.

	Participants with volumetric data				Participants with diffusion data			
	VP, *n* = 91	MP, *n* = 63	LP, *n* = 104	FT, *n* = 70	VP, *n* = 92	MP, *n* = 69	LP, *n* = 120	FT, *n* = 80
Gestational age at birth in weeks, mean (SD), min-max	27.9 (1.4), 24.6 – 29.9	33.0 (0.6), 32.0 – 33.9	35.1 (0.8), 34.0 – 36.9	39.6 (1.3), 37.0 – 42.1	28.0 (1.3), 24.6 – 29.9	33.1 (0.6), 32.0 – 33.9	35.1 (0.8), 34.0 – 36.9	39.6 (1.3), 37.0 – 42.1
Postmenstrual age at MRI in weeks, mean (SD), min-max	42.4 (1.5), 39.0 – 44.6	41.1 (1.2), 38.4 – 43.7	41.6 (1.1), 38.6 – 44.1	42.4 (1.2), 40.3 – 44.9	42.3 (1.5), 39.0 – 44.9	41.2 (1.2), 38.4 – 43.7	41.6 (1.1), 38.6 – 44.1	42.3 (1.3), 39.6 – 44.9
Male, *n* (%)	48 (52.7)	26 (41.3)	47 (45.2)	39 (55.7)	48 (52.2)	32 (46.4)	58 (48.3)	47 (58.8)
Birthweight in grams, mean (SD), min-max	1081 (254), 528 – 1638	1877 (316), 1000 – 2515	2293 (444), 1432 – 4522	3549 (444), 2612 – 4630	1068 (245), 528 – 1630	1917 (348), 1000 – 2670	2313 (449), 1282 – 4522	3588 (469), 2612 – 4630
Birthweight SD score[a], mean (SD)	–0.30 (1.05)	-0.33 (1.03)	-0.40 (1.17)	0.32 (0.81)	-0.35 (1.02)	-0.25 (1.05)	-0.36 (1.20)	0.36 (0.81)
Small for gestational age[b], *n* (%)	6 (6.6)	6 (9.5)	10 (9.6)	0 (0)	7 (7.6)	5 (7.2)	12 (10.0)	0 (0)
Postnatal growth z-score[a], mean (SD)	–0.59 (1.03)[c]	–0.72 (0.84)	–0.49 (0.81)[d]	–0.59 (0.53)[e]	–0.59 (1.05)[f]	–0.74 (0.89)[g]	–0.47 (0.80)[h]	–0.63 (0.52)[i]
Multiple birth, *n* (%)	41 (45.1)	33 (52.4)	34 (32.7)	0 (0)	40 (43.5)	34 (49.3)	36 (30.0)	0 (0)
Respiratory complications[j], *n* (%)	90 (98.9)	20 (31.7)	15 (14.4)	0 (0)[k]	91 (98.9)	22 (31.9)	20 (16.7)	0 (0)[l]
Chronic lung disease, *n* (%)	22 (24.2)	0 (0)	0 (0)	0 (0)	19 (20.7)	0 (0)	0 (0)	0 (0)
Infection[m], *n* (%)	39 (42.9)	3 (4.8)	4 (3.8)	0 (0)	39 (42.4)	3 (4.3)	7 (5.8)	0 (0)
Cystic periventricular leukomalacia[n], *n* (%)	1 (1.1)	0 (0)	0 (0)	0 (0)	1 (1.1)	0 (0)	0 (0)	0 (0)
Intraventricular haemorrhage grade 3 or 4[n], *n* (%)	3 (3.3)	0 (0)	0 (0)	0 (0)	3 (3.3)	0 (0)	0 (0)	0 (0)
Brain abnormality score[o], median (IQR)	4 (3-6)[c]	2 (1-3)	1 (0-2)[d]	1 (0-2)[p]	4 (3-5)[f]	2 (1-3)[g]	1 (0-2)[q]	0 (0-1)[r]
White matter signal abnormalities[o], *n* (%)	8 (9)	5 (8)	4 (4)	2 (3)	9 (10)	5 (7)	4 (3)	2 (3)

FT = full-term; LP = late preterm; MP = moderate preterm; MRI = magnetic resonance imaging; SD = standard deviation; VP = very preterm.
[a]Birth weight SD score was calculated as each infant's weight relative to that expected for sex and gestational age using the British Growth Reference dataset (Cole et al., 1998). Postnatal growth was then calculated as the difference between the weight SD score at birth and at MRI. Some infants are missing data for postnatal growth, because it was not possible to collect weight at MRI data for these infants.[b]Birthweight more than two SDs below the mean birthweight for sex and gestational age;[c]n = 90;[d]n = 103;[e]n = 65;[f]n = 91;[g]n = 68;[h]n = 119;[i]n = 75;[j]Clinical diagnosis of transient tachypnoea of the newborn, respiratory distress of the newborn, pneumothorax or pneumonia;[k]n = 37;[l]n = 48;[m]Suspected or proven sepsis and/or necrotising enterocolitis;[n]Cystic periventricular leukomalacia and intraventricular haemorrhage were diagnosed from cranial ultrasound images obtained prior to term-equivalent age in infants born < 30 weeks' gestational age only. More mature infants were scanned only if clinically indicated, which was rare. Intraventricular haemorrhage was graded according to Papile et al., 1978;[o]Term-equivalent MRI were scored using a standardised scoring system (Kidokoro et al., 2013; Walsh et al., 2014). White matter signal abnormalities included focal punctate, extensive punctate, and/or linear signal intensity abnormalities;[p]n = 67;[q]n = 115;[r]n = 77.

in Table 1. The postmenstrual age at MRI of the MP and LP infants was on average a week younger than that of the VP infants. Rates of major brain injuries in the neonatal period were low in all GA groups. Only three infants in our study had major neonatal brain injuries; one VP infant had cystic periventricular leukomalacia (PVL) and intraventricular hemorrhage (IVH) grade three in both hemispheres, and two VP infants had IVH grade three (one had grade three in both hemispheres, and one had IVH grade three in the left hemisphere and grade two in the right hemisphere).

Compared with the larger cohort of eligible infants (n = 551), the

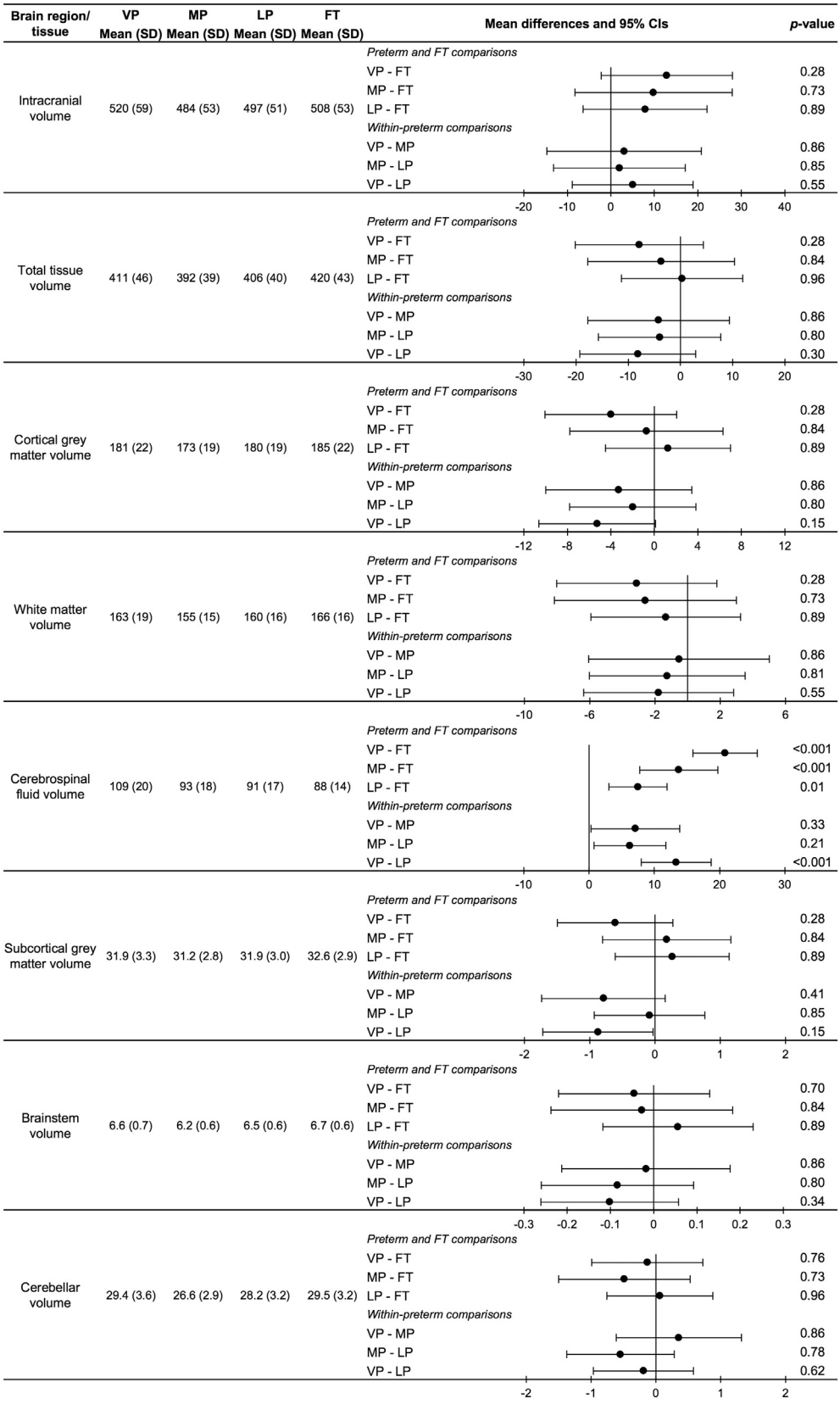

Fig. 2. Results of the global brain volume analysis.
The values are the raw means and standard deviations (SD) for each gestational age group and brain region. The plots are the mean differences and 95% confidence intervals (CI) between gestational age groups for each brain region, adjusted for postmenstrual age at time of scan. Full-term (FT); late preterm (LP); moderate preterm (MP); and very preterm (VP).
For the plots, each row is one group compared with another group, for example VP compared with the FT group (VP-FT). The first named group (VP) is the group of interest; the second named group (FT) is the reference group. Points to the right of the zero line indicate the volume is smaller in the group of interest (VP) compared with the reference group (FT); points to the left of the zero line indicate the volume is larger in the group of interest (VP) compared with the reference group (FT).
False discovery rate-corrected p-values are shown.
Volume units are cm^3.

participants with volumetric (n = 328) and diffusion (n = 361) data had a lower GA at birth and birthweight, were more likely to be a multiple birth or to have had antenatal corticosteroids, and were less likely to have had patent ductus arteriosus or respiratory complications (all $p \leq .001$).

3.2. Comparisons of global brain volumes between the gestational age groups

Raw means and SDs for each of the global brain volumes in each of the GA groups are presented in Fig. 2. Mean differences in global brain volumes between the GA groups are also shown. There was little evidence for an effect of GA group on total intracranial (p = .6), total tissue (p = .6), white matter (p = .6), cortical grey matter (p = .6), brainstem (p = .6), cerebellum (p = .6) or subcortical grey matter volumes (p = .6) (Fig. 2). However, there was evidence of an overall effect of GA group on cerebrospinal fluid volume ($p < .001$), with post-hoc tests revealing that all preterm groups had larger cerebrospinal fluid volume than the FT group. The magnitude of the difference was greatest for VP compared with FT infants, then for MP compared with FT infants, and then for LP compared with FT infants. Within the preterm group, the VP sub-group had larger cerebrospinal fluid volume than the

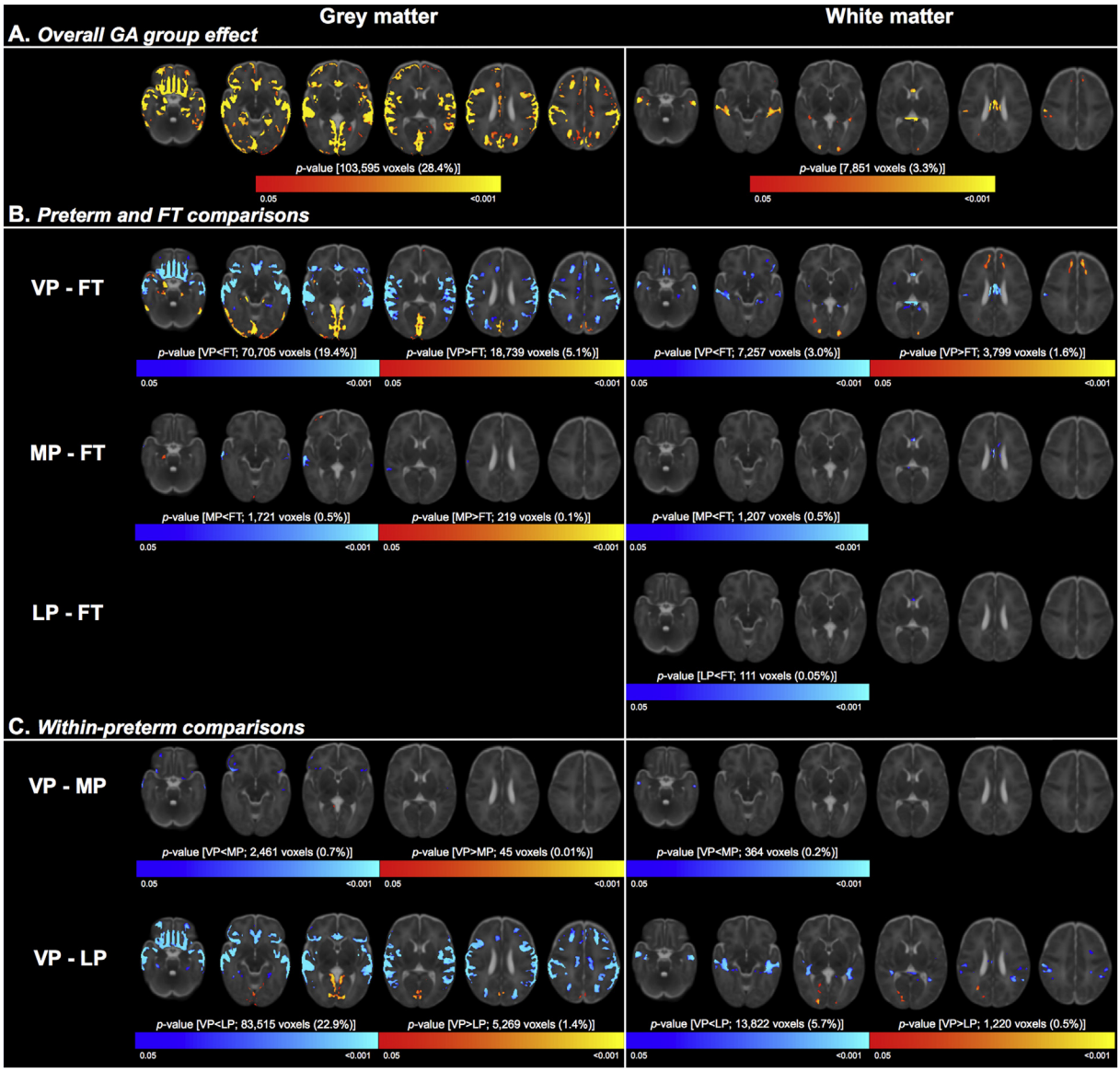

Fig. 3. Results of the regional volume analysis.
Part A shows the overall effect of gestational age (GA) group on regional grey (left column) and white (right column) matter volumes, adjusted for postmenstrual age at time of scan. The clusters where there was evidence that the brain measures differed between the four GA groups are shown in red-yellow, overlaid on the T2 template.
Part B shows the directional differences between each preterm group and the full-term (FT) group. Clusters that were larger in each preterm group compared with the FT group are red-yellow; clusters that were smaller in each preterm group compared with the FT group are blue-light blue.
Part C shows the directional differences between the preterm sub-groups [very (VP), moderate (MP) and late (LP) preterm]. Clusters that were larger in the VP group compared with the MP or LP group are red-yellow; clusters that were smaller in the VP group compared with the MP or LP group are blue-light blue.
In each part, the number of significant voxels and their % of the total cortical grey matter (365,236 voxels) or white matter (240,905 voxels) volume are also reported.
TFCE = threshold free cluster enhancement. FWE = family-wise error rate. (For interpretation of the references to color in this figure legend, the reader is referred to the web version of this article.)

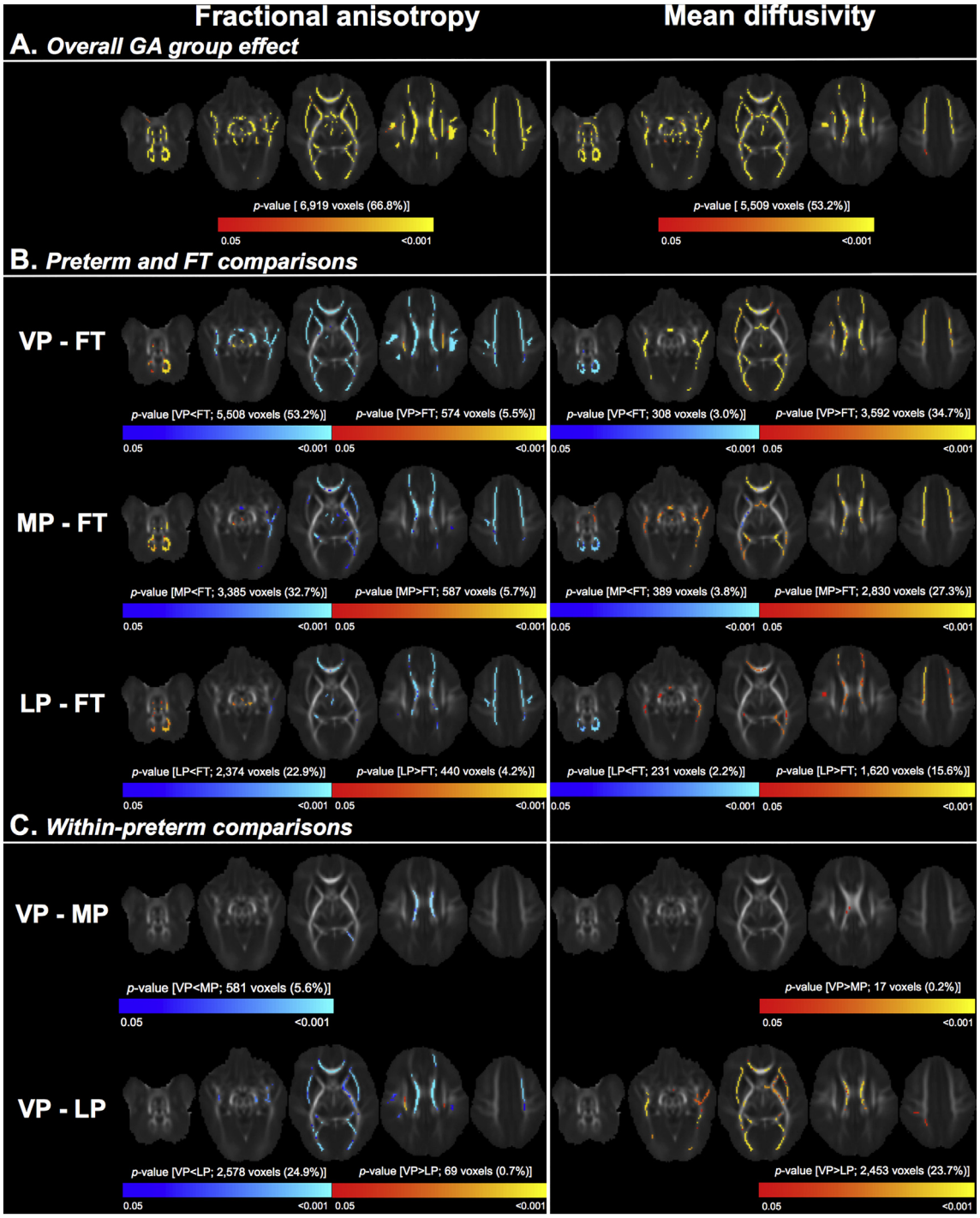

Fig. 4. Results of the regional microstructural analysis.
Part A shows the overall effect of gestational age (GA) group on fractional anisotropy (left column) and mean diffusivity (right column), adjusted for postmenstrual age at time of scan. The clusters where there was evidence that the diffusion measures differed between the four GA groups are shown in red-yellow, overlaid on the mean fractional anisotropy image.
Part B shows the directional differences between each preterm group and the full-term (FT) group. Clusters that had higher values in each preterm group compared with the FT group are red-yellow; clusters that had lower values in each preterm group compared with the FT group are blue-light blue.
Part C shows the directional differences between the preterm sub-groups [very (VP), moderate (MP) and late (LP) preterm]. Clusters that had higher values in the VP group compared with the MP or LP group are red-yellow; clusters that had lower values in the VP group compared with the MP or LP group are blue-light blue.
In each part, the number of significant voxels and their % of the total mean fractional anisotropy skeleton (10,361 voxels) are also reported.
TFCE = threshold free cluster enhancement. FWE = family-wise error rate. (For interpretation of the references to color in this figure legend, the reader is referred to the web version of this article.)

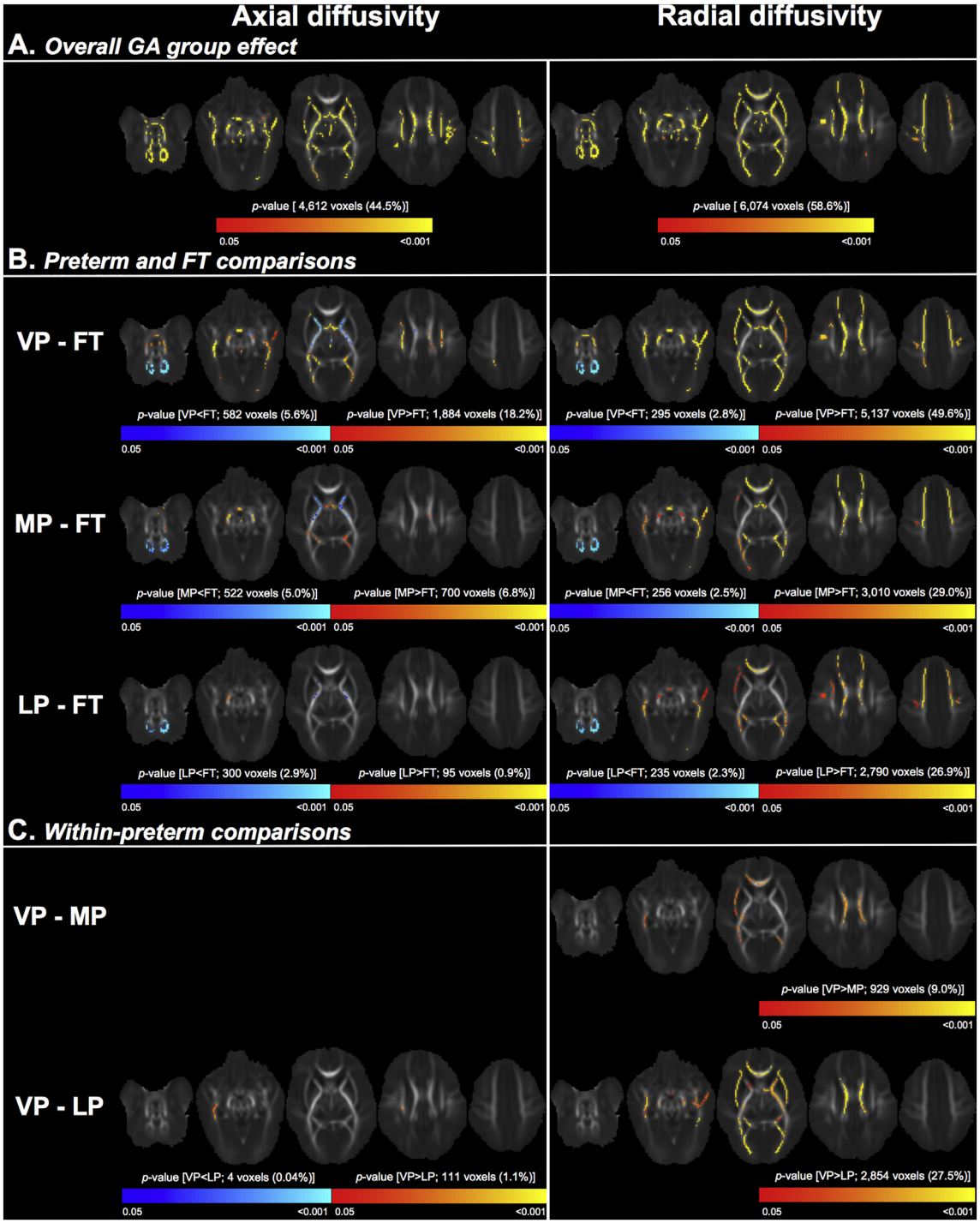

Fig. 5. Results of the regional microstructural analysis (continued).
Part A shows the overall effect of gestational age (GA) group on axial diffusivity (left column) and radial diffusivity (right column), adjusted for postmenstrual age at time of scan. The clusters where there was evidence that the diffusion measures differed between the four GA groups are shown in red-yellow, overlaid on the mean fractional anisotropy image.
Part B shows the directional differences between each preterm group and the full-term (FT) group. Clusters that had higher values in each preterm group compared with the FT group are red-yellow; clusters that had lower values in each preterm group compared with the FT group are blue-light blue.
Part C shows the directional differences between the preterm sub-groups [very (VP), moderate (MP) and late (LP) preterm]. Clusters that had higher values in the VP group compared with the MP or LP group are red-yellow; clusters that had lower values in the VP group compared with the MP or LP group are blue-light blue.
In each part, the number of significant voxels and their % of the total mean fractional anisotropy skeleton (10,361 voxels) are also reported.
TFCE = threshold free cluster enhancement. FWE = family-wise error rate. (For interpretation of the references to color in this figure legend, the reader is referred to the web version of this article.)

LP sub-group. The magnitude of within-preterm group differences was smaller than the magnitude of between-preterm and FT group differences (Fig. 2).

3.3. Comparisons of regional brain volumes between the gestational age groups

VBM showed that GA group was associated with volume in sub-regions (~28%) of the total cortical grey matter, located throughout the occipital, temporal, parietal and frontal lobes. GA group was also associated with volume in sub-regions (~3%) of the total white matter, particularly in the white matter in the temporal lobe and corpus callosum. The regions where GA group was associated with cortical grey matter and white matter volumes are pictured in Fig. 3A and listed in Supplementary Table 1.

Post-hoc analyses showed that the overall effect of GA group on cortical grey matter and white matter volumes was mostly driven by differences between the VP and FT groups (Fig. 3B, Supplementary Table 1). The VP group had many regions of smaller cortical grey matter volume than the FT group, located throughout the frontal, temporal and parietal lobes, and some regions of smaller white matter volume than the FT group, located mostly in the corpus callosum and temporal white matter. The MP group also had some regions of smaller cortical grey matter volume than the FT group, located in the temporal lobe, and smaller white matter volume than the FT group, located in the corpus callosum. However, the differences between the MP and FT group were less widespread throughout the brain compared with the differences between the VP and FT groups. There were also differences in white matter volume between the LP and FT groups, but these were even less widespread than the differences between the MP and FT groups; the LP group only had smaller white matter volume than the FT group in a small part of the corpus callosum. There were no differences in cortical grey matter volume between the LP and FT group (Fig. 3B, Supplementary Table 1).

There were also some regions where the preterm groups had *larger* volume than the FT group. The VP group had larger cortical grey matter volume than the FT group in parts of the occipital and temporal lobes, and larger white matter volume than the FT group in parts of the occipital and frontal white matter. The MP group had larger cortical grey matter volume than the FT group in small parts of the occipital and temporal lobes; this difference was much less widespread than the difference between the VP and FT groups. The LP group had no regions of larger volume than the FT group (Fig. 3B, Supplementary Table 1).

Within the preterm group, the VP sub-group had smaller volume than the MP sub-group in the frontal and temporal grey matter and the temporal white matter. The VP sub-group also had many regions of smaller cortical grey matter volume (located throughout the frontal, parietal and temporal lobes), several regions of smaller white matter volume (located predominantly in the temporal white matter), and some regions of larger cortical grey matter and white matter volume (located predominantly in the occipital lobe), compared with the LP sub-group. However, there were no regions in the cortical grey matter or white matter where volume differed between the MP and LP sub-groups (Fig. 3C, Supplementary Table 1).

3.4. Comparisons of regional white matter microstructure between the gestational age groups

TBSS showed that GA group was associated with FA, MD, AD and RD in much of the white matter (45–67% of the mean FA skeleton), as pictured in Figs. 4A and 5A, and listed in Supplementary Tables 2 and 3. The regions in which GA group was associated with FA, MD, AD and RD overlapped with some of the regions in which GA group was associated with white matter volume. The overlapping regions were in voxels in the approximate location of the corpus callosum, fornix, occipital white matter (including posterior thalamic radiation and sagittal stratum), and temporal white matter. An example of the overlap is shown in Supplementary Fig. 1.

Post-hoc analyses showed that the VP group had lower FA and higher MD than the FT group in many voxels, which were located throughout the white matter (visualised in Fig. 4B and listed in Supplementary Table 2). The MP group also had lower FA and higher MD than the FT group in many voxels throughout much of the white matter. These voxels were in similar locations to those in the VP-FT comparison, but the overall percentage of voxels that differed between the MP and FT groups was ~10–20% fewer than in the VP-FT comparison, and the strength of the FA and MD differences between the MP and FT groups was weaker than between the VP and FT groups (as evidenced by the change in the colour-coded *p*-values in Fig. 4B). Similarly, the LP group had lower FA and higher MD than the FT group, but the overall percentage of voxels that differed between the LP and FT groups was ~10–20% fewer than in the MP-FT comparison, and the strength of the differences between the LP and FT groups was weaker than between the MP and FT groups (Fig. 4B, Supplementary Table 2).

There was also a small number of voxels that showed the opposite pattern; they had higher FA and lower MD in each preterm group compared with the FT group. These voxels were mostly in the approximate location of the cerebellar and brainstem white matter, and the cerebral peduncle, internal capsule and corona radiata. The number of voxels that had this opposite pattern was relatively stable between the comparisons of the VP group with the FT group, the MP group with the FT group and the LP group with the FT group; i.e. ~2–5% of the skeleton had lower FA or higher MD in each preterm sub-group compared with the FT group (Fig. 4B, Supplementary Table 2).

The differences in FA and MD between each preterm group and the FT group were mostly driven by RD rather than AD. There were many voxels, located throughout much of the white matter, that had higher RD in each preterm sub-group compared with the FT group. The number of voxels that had higher RD progressively decreased from the VP-FT comparison through to the LP-FT comparison (Fig. 5B, Supplementary Table 3). There was also a small number of voxels (~2% of the skeleton) that had lower RD in each preterm group compared with the FT group, located in the cerebellar white matter (Fig. 5B, Supplementary Table 3).

Compared with the RD differences between the preterm and FT groups, the AD differences between groups were slightly more variable; fewer voxels had higher AD, and more voxels had lower AD, in each preterm group compared with the FT group. These voxels with higher AD were less widespread than the voxels with higher RD. The voxels with lower AD were in the approximate location of the cerebellar and brainstem white matter, as well as the cerebral peduncle, internal capsule, and corpus callosum (Figure 5, Supplementary Table 3).

Within the preterm groups, there were some voxels that had lower FA and higher MD and RD in the VP sub-group compared with the MP sub-group, mostly in the approximate location of the corpus callosum. There were many voxels that had lower FA and higher MD and RD in the VP sub-group compared with the LP sub-group, located throughout much of the white matter. There were also a small number of voxels that had *higher* FA in the VP group compared with the LP sub-group, in the approximate location of the corona radiata. There were no differences in AD between the VP and MP sub-groups, and only a small number of voxels in which AD differed between the VP and LP sub-groups. There were also no differences in diffusion tensor measures between the MP and LP sub-groups (Figs. 4C and 5C, Supplementary Tables 2 and 3).

4. Discussion

In summary, cerebrospinal fluid volume was larger in all preterm sub-groups compared with the FT group, and volume was smaller in parts of the temporal cortical grey matter, and parts of the temporal white matter and corpus callosum, in all preterm sub-groups compared

with the FT group. FA was lower and RD and MD were higher in much of the white matter in all preterm sub-groups compared with the FT group. The anatomical locations of group differences were relatively constant between the VP, MP and LP comparisons with the FT group, but the magnitude and spatial extent of group differences was largest for the VP, followed by the MP, and then the LP comparisons. Within the preterm group, the VP sub-group had smaller frontal and temporal grey and white matter volume, and lower FA and higher MD and RD in voxels in the approximate location of the corpus callosum compared with the MP sub-group. However, there were few volume and microstructural differences between the MP and LP sub-groups.

The finding that preterm groups have larger cerebrospinal fluid volume than the FT group at TEA is consistent with previous research in VP groups (Boardman et al., 2006; Inder et al., 2005; Keunen et al., 2012; Mewes et al., 2006; Padilla et al., 2015; Thompson et al., 2007). The magnitude of our difference in cerebrospinal fluid volume between VP and FT groups (~20 cm^3) was similar to these previous studies (~17 cm^3 in Inder et al., 2005; ~20 cm^3 in Thompson et al., 2007; ~27.5 in Mewes et al., 2006). Our study has additionally established that MP and LP sub-groups both have larger cerebrospinal fluid volume than the FT group at TEA, although the magnitude of these differences was smaller than the magnitude of the VP difference. One other study also reported that LP children have larger cerebrospinal fluid volume than FT children at 6–13 years of age (Brumbaugh et al., 2016), so it is possible that our finding at TEA will persist into childhood. However, other global volumes, including total tissue, cortical grey matter, white matter, deep nuclear grey matter, cerebellum, and brainstem, did not differ between the GA groups at TEA. This was unexpected given many previous studies have found that VP groups have smaller brain tissue volumes than FT groups at TEA (Boardman et al., 2006; Inder et al., 2005; Keunen et al., 2012; Mewes et al., 2006; Padilla et al., 2015; Srinivasan et al., 2007; Thompson et al., 2007).

In contrast to the lack of global brain tissue volume differences between GA groups, on regional analysis parts of the cortical grey matter and white matter had smaller volume in all the preterm groups compared with the FT group. The regions that had smaller cortical grey matter and white matter in the VP than the FT group included frontal, temporal and parietal grey matter, and corpus callosum and temporal white matter, which is consistent with some previous studies (Padilla et al., 2015; Peterson et al., 2003; Thompson et al., 2011; Thompson et al., 2007). Our regional analysis also established that MP and LP sub-groups have some regions of smaller cortical grey matter and/or white matter compared with the FT group at TEA, located in the temporal grey matter and corpus callosum for the MP group, and the corpus callosum for the LP group. While we found that our LP group had smaller white matter volume in the corpus callosum than the FT group, the only other research on LP groups has found they have smaller *grey* matter volume compared with FT groups, including smaller total grey matter at TEA (Munakata et al., 2013), and smaller temporal grey matter in childhood (Rogers et al., 2014). The reason for this discrepancy is unclear and warrants future investigation, but it could be related to differences in clinical or demographic characteristics between studies, with the previous studies having smaller sample sizes and different ages at MRI compared with the current study.

On regional microstructural analysis, we found that all preterm groups had lower FA and higher MD throughout much of the white matter compared with the FT group. The lower FA and higher MD was mostly driven by higher RD rather than AD. Our differences between VP and FT groups are consistent with previous research, which has commonly found that VP groups have lower FA and higher RD and MD in many major tracts compared with FT groups [(Alexandrou et al., 2014; Anjari et al., 2007; Ball et al., 2013; Pogribna et al., 2013; Rose et al., 2008); for a review see (Anderson et al., 2015; Pandit et al., 2013)]. The only other study that has investigated white matter microstructure in MP and LP groups is our previous TBSS study on the same cohort of infants as the current study, in which we similarly found that the combined MP and LP infants have lower FA and higher MD, AD and RD throughout much of the white matter compared with the FT group at TEA (Kelly et al., 2016). The current study builds upon our previous study by examining infants born across the wider GA spectrum; i.e. the MP and LP groups separately in relation to the FT group, and the MP and LP groups in relation to the VP group. These are both important advances given the known differing clinical risks of the VP, MP, LP and FT groups (Ancel et al., 2015; Manuck et al., 2016).

Unexpectedly, some parts of the cortical grey matter and white matter, particularly in the occipital and temporal lobes, had *larger* volume in the preterm groups compared with the FT group. This unexpected finding challenges conventional findings in VP groups, but does line up with some other recent studies. One study found that younger GA at birth was associated with larger volume of all brain tissues (grey matter, white matter, cerebrospinal fluid and cerebellum) in ~800 infants born between 27 and 42 weeks' GA and scanned between 37 and 57 weeks' GA (Knickmeyer et al., 2016). Another study found that preterm infants had smaller volumes in temporal cortical regions, deep grey matter, cerebellum and brainstem, but also increased grey matter and white matter volumes in occipital, parietal and frontal regions, compared with FT infants at TEA (Padilla et al., 2015). Similarly, some white matter regions unexpectedly had *higher* FA and *lower* MD and RD in the preterm groups compared with the FT group, mainly in the cerebellar and brainstem white matter, as previously reported (Brossard-Racine et al., 2017; Kaur et al., 2014; Kelly et al., 2016), but also sometimes in the cerebral peduncles, corona radiata, internal capsule, and corpus callosum, similar to another study that found higher FA in preterm infants compared with FT infants in corticospinal projection tracts (Rose et al., 2008). One explanation for these unexpected volume and microstructural findings is that larger volumes, and higher FA and lower MD and RD, could reflect accelerated development of certain brain regions in the preterm groups compared with the FT group. This could be due to longer exposure to visual or sensorimotor stimuli in the extrauterine environment in the preterm groups compared with the FT group (Gimenez et al., 2008; Knickmeyer et al., 2016). However, it is also known that diffusion tensor findings are difficult to interpret in crossing fibre regions (Dubois et al., 2014; Jones et al., 2013; Rose et al.).

There was consistency between our volume and microstructural findings, with some of the regions that had lower volume also having altered microstructure, including the corpus callosum, and occipital and temporal white matter. In both the volume and microstructural analysis, atypical volume and microstructure when compared with the FT group was most pronounced for the VP group, less pronounced for the MP group, and least pronounced for the LP group. This finding is consistent with the known clinical risks of these GA groups; risk of perinatal morbidities and neurodevelopmental impairments is highest in VP infants, and lower in MP and LP infants, but still higher in all preterm groups compared with FT groups (Altman et al., 2011; Ancel et al., 2015; Cheong et al., 2017; Lindstrom et al., 2011; Manuck et al., 2016; Moster et al., 2008; Teune et al., 2011; Yaari et al., 2018). Thus, the current study aids in understanding the neural basis of the different clinical risks between GA groups.

There was a discrepancy between the results of our global and regional analyses, in that differences in regional cortical grey and white matter volumes between the preterm and FT groups were found, but no differences in global cortical grey and white matter volumes between groups were found. There are several possible explanations. For regional cortical grey matter analyses, we found both regions of smaller volume and regions of larger volume in the preterm groups compared with the FT group, which may have cancelled each other out, resulting in the lack of differences in global cortical grey matter volume. The regions that had smaller white matter volume in the preterm groups compared with the FT group made up only a small percentage of the total white matter volume (a maximum of 3%), which might have washed out when analysing global white matter volume. It is possible

that the regional analyses might have uncovered subtler differences between GA groups, i.e. more localised regions that are more vulnerable (have smaller volume) or more developed (have larger volume) than other regions in the preterm groups compared with the FT group. These regional findings might be important as they might have implications for later functioning in specific cognitive, motor, or behavioural domains that are reportedly adversely affected in preterm children (Cheong et al., 2017). However, there may also be methodological explanations for the discrepancy. One possibility is that the results from VBM may be influenced by cerebrospinal fluid volume, given the proximity of the cortical ribbon to the cerebrospinal fluid, and the large differences we found in cerebrospinal fluid volume between GA groups. More detailed examination of 100 brain regions (Alexander et al., 2017) is underway in our cohort, and may help to validate the reliability of the current results from VBM.

Within the preterm group, the VP sub-group had many differences to the LP sub-group, including larger cerebrospinal fluid volume, smaller cortical grey matter volume throughout the frontal, parietal and temporal lobes, smaller temporal white matter volume, and lower FA and higher MD and RD in much of the white matter. The magnitude and spatial extent of the differences between the VP and LP sub-groups was generally quite similar to that between the VP and FT sub-groups. The VP sub-group also had smaller frontal grey matter volume, smaller temporal white matter volume, and lower FA and higher MD and RD in voxels in the approximate location of the corpus callosum, compared with the MP sub-group. This suggests that, as expected, the VP sub-group has particular brain vulnerabilities compared with other preterm sub-groups. The particular vulnerability of the frontal grey matter may line up with the known central-to-peripheral and posterior-to-anterior sequence of brain development, where frontal regions are the last to develop (Oishi et al., 2011), and these regions may therefore be more vulnerable in infants born earlier. Particular vulnerability of the corpus callosum in VP groups also lines up with previous studies (Li et al., 2015; Thompson et al., 2011). There was little evidence of regional volume and microstructural differences between the MP and LP sub-groups. While each of the MP and LP groups separately had regional volume and microstructural differences to the FT group, they do not appear to differ substantially from each other in regional volumes or microstructure. This might relate to the wider gap in the mean GA at birth between the VP and MP groups (5 weeks) compared with between the MP and LP groups (2 weeks).

There are some limitations regarding our cohort. The MP and LP infants were scanned on average a week earlier than the VP infants, as infants who are well are discharged earlier from hospital. Despite adjusting for postmenstrual age at scan, the full effects of being born MP and LP relative to VP and FT may not be evident from this study. It is important that future studies of brain development tightly monitor age at scan in infant cohorts that are undergoing a period of rapid brain development, to avoid the possibility of confounding results. Another limitation is that our study sample may not be fully representative of the preterm population, as those included in the imaging sample had a lower GA at birth and birthweight, were more likely to be a multiple birth and to have had antenatal corticosteroids, and were less likely to have had a patent ductus arteriosus or respiratory distress than the larger sample that was recruited. Additionally, our VP group was also a relatively 'low-risk' group considering the low rate of brain injury in our infants compared with other VP populations reported in the literature. A further limitation is that infants born at 30–31 weeks' GA were not represented in this study, due to the sample being derived from two separate cohorts with different GA inclusion criteria (Spittle et al., 2014; Walsh et al., 2014).

There are also some limitations regarding our MRI analyses. There is a large range of possible MRI analysis techniques available, and we aimed to use commonly adopted techniques to characterise brain volume and microstructure in the clinically important GA groups and to generate information that is readily comparable with other clinical research studies. Despite the wide use of VBM and TBSS, these techniques have known limitations, as detailed previously (Bach et al., 2014; Scarpazza et al., 2015). Notably, both TBSS and VBM results are heavily dependent on accurate segmentation and registration, particularly in the presence of image distortions and the variable structure of preterm and FT infant brains. Some studies have discussed the associated registration problems and potential solutions (Schwarz et al., 2014; Van Hecke et al., 2007). Specific to TBSS is the fact that the skeletonisation step introduces a spatial variability and orientational heterogeneity of the statistical sensitivity which may limit the reliability and interpretation of our results (Edden and Jones, 2011). An additional drawback of confining the spatial location of the analysis to a skeleton is the lack of specificity (Jones and Cercignani, 2010). For example, in regions where multiple fibre structures converge such as the interface of the superior parts of the corpus callosum and the corticospinal tracts, the skeleton cannot be defined unambiguously (Van Hecke et al., 2010). Another consideration in TBSS analyses is the use of a study-specific target image, which was initially recommended as part of the TBSS pipeline, as it may provide more successful registrations than an average template (Smith et al., 2006), but could also introduce bias if one GA group better matches the selected image. Some studies have shown that the use of an average template outperforms a study-specific target image (Bach et al., 2014; Keihaninejad et al., 2012) and could be used to improve TBSS analyses in future studies. We corrected for echo planar imaging distortions in the diffusion images using an average field map because field maps were not acquired for all infants, and while we found that this correction improved the image distortions, future studies should acquire field maps or reversed phase-encode images for all infants. Future studies using techniques that focus on cortical sub-regions (Alexander et al., 2017) or specific tracts (Pecheva et al., 2017; Thompson et al., 2011) will be highly valuable to further refine our understanding of the possible brain vulnerabilities of the different GA groups. In the case of diffusion MRI, there is not only a range of possible analysis techniques, but also a range of possible measures. The most common measures- FA, AD, RD and MD- are obtained from the diffusion tensor imaging model and provide a sensitive but non-specific reflection of the white matter microstructural environment (Jones et al., 2013). Other measures may be used in future that may be more specific to the underlying cellular properties from more advanced models (Assaf and Basser, 2005; Raffelt et al., 2017; Zhang et al., 2012). However, these advanced models tend to require diffusion acquisitions with higher *b*-values and a larger number of gradient directions than required for diffusion tensor imaging, and such acquisitions are more challenging to obtain in clinical settings, particularly when scanning neonates. A next step will be to use advanced machine learning techniques (Ball et al., 2016) to examine whether brain structure at TEA can predict the developmental status of individual infants. Additionally, in the current study we analysed several different modalities and measures separately. Future studies using alternative approaches would be valuable, for example multivariate or data reduction approaches, which would enable joint inference over multiple modalities (Telford et al., 2017; Winkler et al., 2016). Another crucial future step will be to examine whether the brain structural differences between GA groups in the current study at TEA are associated with longer-term neurodevelopmental outcomes.

In conclusion, this study has characterised brain structure at TEA in clinically important GA groups. Our major findings were that all preterm sub-groups had atypical brain volume and microstructure at TEA when compared with the FT group. In general, the groups followed a gradient, whereby all preterm sub-groups differed to the FT group in similar anatomical regions (particularly cerebrospinal fluid, temporal grey and white matter, and corpus callosum), but the differences were most pronounced for the VP group, less pronounced for the MP group, and least pronounced for the LP group. Additionally, within the preterm group, the VP sub-group had specific vulnerability of the frontal and temporal grey and white matter and corpus callosum, while the MP and

LP sub-groups did not differ substantially from each other. This study provides information to help understand the possible neural basis for the different clinical risks of the GA sub-groups. Our findings add to the growing body of evidence of the vulnerabilities of MP and LP groups when compared with FT groups (Cheong et al., 2017), and further support the need for increased surveillance and early intervention in MP and LP infants, in addition to VP infants. Identifying which infants are at higher risk for particular brain abnormalities early in life, while there is still large potential for neuroplasticity, may enable clinicians to target infants requiring increased developmental surveillance who might benefit from new neuroprotective and neurorestorative strategies.

Supplementary data to this article can be found online at https://doi.org/10.1016/j.nicl.2018.101630.

Acknowledgements

We gratefully acknowledge support from members of the Victorian Infant Brain Studies (VIBeS) group, Developmental Imaging group, and Melbourne Children's MRI Centre at the Murdoch Children's Research Institute, and thank the families who participated in the study. This work was supported in part by the Australian National Health and Medical Research Council (NHMRC) (Project Grant ID 1028822 and 1024516; Centre of Clinical Research Excellence Grant ID 546519; Centre of Research Excellence Grant ID 1060733; Senior Research Fellowship ID 1081288 to P.J.A.; Early Career Fellowship ID 1053787 to J.L.Y.C., ID 1053767 to A.J.S., ID 1012236 to D.K.T.; Career Development Fellowship ID 1108714 to A.J.S., ID 1085754 to D.K.T.), Murdoch Children's Research Institute Clinical Sciences Theme Grant, the Royal Children's Hospital, the Department of Paediatrics at the University of Melbourne, the Victorian Government Operational Infrastructure Support Program, and The Royal Children's Hospital Foundation.

References

Alexander, B., Murray, A.L., Loh, W.Y., Matthews, L.G., Adamson, C., Beare, R., Chen, J., Kelly, C.E., Rees, S., Warfield, S.K., Anderson, P.J., Doyle, L.W., Spittle, A.J., Cheong, J.L., Seal, M.L., Thompson, D.K., 2017. A new neonatal cortical and subcortical brain atlas: the Melbourne children's regional infant brain (M-CRIB) atlas. NeuroImage 147, 841–851.

Alexandrou, G., Martensson, G., Skiold, B., Blennow, M., Aden, U., Vollmer, B., 2014. White matter microstructure is influenced by extremely preterm birth and neonatal respiratory factors. Acta Paediatr. 103, 48–56.

Altman, M., Vanpee, M., Cnattingius, S., Norman, M., 2011. Neonatal morbidity in moderately preterm infants: a Swedish national population-based study. J. Pediatr. 158 (239–244), e231.

Ancel, P.Y., Goffinet, F., Group, E.-W, Kuhn, P., Langer, B., Matis, J., Hernandorena, X., Chabanier, P., Joly-Pedespan, L., Lecomte, B., Vendittelli, F., Dreyfus, M., Guillois, B., Burguet, A., Sagot, P., Sizun, J., Beuchee, A., Rouget, F., Favreau, A., Saliba, E., Bednarek, N., Morville, P., Thiriez, G., Marpeau, L., Marret, S., Kayem, G., Durrmeyer, X., Granier, M., Baud, O., Jarreau, P.H., Mitanchez, D., Boileau, P., Boulot, P., Cambonie, G., Daude, H., Bedu, A., Mons, F., Fresson, J., Vieux, R., Alberge, C., Arnaud, C., Vayssiere, C., Truffert, P., Pierrat, V., Subtil, D., D'Ercole, C., Gire, C., Simeoni, U., Bongain, A., Sentilhes, L., Roze, J.C., Gondry, J., Leke, A., Deiber, M., Claris, O., Picaud, J.C., Ego, A., Debillon, T., Poulichet, A., Coline, E., Favre, A., Flechelles, O., Samperiz, S., Ramful, D., Branger, B., Benhammou, V., Foix-L'Helias, L., Marchand-Martin, L., Kaminski, M., 2015. Survival and morbidity of preterm children born at 22 through 34 weeks' gestation in France in 2011: results of the EPIPAGE-2 cohort study. JAMA Pediatr. 169, 230–238.

Anderson, P.J., Cheong, J.L., Thompson, D.K., 2015. The predictive validity of neonatal MRI for neurodevelopmental outcome in very preterm children. Semin. Perinatol. 39, 147–158.

Anjari, M., Srinivasan, L., Allsop, J.M., Hajnal, J.V., Rutherford, M.A., Edwards, A.D., Counsell, S.J., 2007. Diffusion tensor imaging with tract-based spatial statistics reveals local white matter abnormalities in preterm infants. NeuroImage 35, 1021–1027.

Ashburner, J., Friston, K.J., 2000. Voxel-based morphometry–the methods. NeuroImage 11, 805–821.

Assaf, Y., Basser, P.J., 2005. Composite hindered and restricted model of diffusion (CHARMED) MR imaging of the human brain. NeuroImage 27, 48–58.

Bach, M., Laun, F.B., Leemans, A., Tax, C.M., Biessels, G.J., Stieltjes, B., Maier-Hein, K.H., 2014. Methodological considerations on tract-based spatial statistics (TBSS). NeuroImage 100, 358–369.

Ball, G., Aljabar, P., Arichi, T., Tusor, N., Cox, D., Merchant, N., Nongena, P., Hajnal, J.V., Edwards, A.D., Counsell, S.J., 2016. Machine-learning to characterise neonatal functional connectivity in the preterm brain. NeuroImage 124, 267–275.

Ball, G., Boardman, J.P., Aljabar, P., Pandit, A., Arichi, T., Merchant, N., Rueckert, D., Edwards, A.D., Counsell, S.J., 2013. The influence of preterm birth on the developing thalamocortical connectome. Cortex 49, 1711–1721.

Beare, R.J., Chen, J., Kelly, C.E., Alexopoulos, D., Smyser, C.D., Rogers, C.E., Loh, W.Y., Matthews, L.G., Cheong, J.L., Spittle, A.J., Anderson, P.J., Doyle, L.W., Inder, T.E., Seal, M.L., Thompson, D.K., 2016. Neonatal brain tissue classification with morphological adaptation and unified segmentation. Front Neuroinform 10, 12.

Blencowe, H., Cousens, S., Chou, D., Oestergaard, M., Say, L., Moller, A.B., Kinney, M., Lawn, J., Born Too Soon Preterm Birth Action, G, 2013. Born too soon: the global epidemiology of 15 million preterm births. Reprod Health 10 (Suppl. 1), S2.

Boardman, J.P., Counsell, S.J., Rueckert, D., Kapellou, O., Bhatia, K.K., Aljabar, P., Hajnal, J., Allsop, J.M., Rutherford, M.A., Edwards, A.D., 2006. Abnormal deep grey matter development following preterm birth detected using deformation-based morphometry. NeuroImage 32, 70–78.

Brossard-Racine, M., Poretti, A., Murnick, J., Bouyssi-Kobar, M., McCarter, R., du Plessis, A.J., Limperopoulos, C., 2017. Cerebellar microstructural organization is altered by complications of premature birth: a case-control study. J. Pediatr. 182, 28–33.

Brumbaugh, J.E., Conrad, A.L., Lee, J.K., Devolder, I.J., Zimmerman, M.B., Magnotta, V.A., Axelson, E.D., Nopoulos, P.C., 2016. Altered brain function, structure, and developmental trajectory in children born late preterm. Pediatr. Res. 80, 197–203.

Cheong, J.L., Doyle, L.W., Burnett, A.C., Lee, K.J., Walsh, J.M., Potter, C.R., Treyvaud, K., Thompson, D.K., Olsen, J.E., Anderson, P.J., Spittle, A.J., 2017. Association between moderate and late preterm birth and neurodevelopment and social-emotional development at age 2 years. JAMA Pediatr. 171, e164805.

Dubois, J., Dehaene-Lambertz, G., Kulikova, S., Poupon, C., Huppi, P.S., Hertz-Pannier, L., 2014. The early development of brain white matter: a review of imaging studies in fetuses, newborns and infants. Neuroscience 276, 48–71.

Edden, R.A., Jones, D.K., 2011. Spatial and orientational heterogeneity in the statistical sensitivity of skeleton-based analyses of diffusion tensor MR imaging data. J. Neurosci. Methods 201, 213–219.

Engle, W.A., 2006. A recommendation for the definition of “late preterm” (near-term) and the birth weight-gestational age classification system. Semin. Perinatol. 30, 2–7.

Gimenez, M., Miranda, M.J., Born, A.P., Nagy, Z., Rostrup, E., Jernigan, T.L., 2008. Accelerated cerebral white matter development in preterm infants: a voxel-based morphometry study with diffusion tensor MR imaging. NeuroImage 41, 728–734.

Huppi, P.S., Maier, S.E., Peled, S., Zientara, G.P., Barnes, P.D., Jolesz, F.A., Volpe, J.J., 1998. Microstructural development of human newborn cerebral white matter assessed in vivo by diffusion tensor magnetic resonance imaging. Pediatr. Res. 44, 584–590.

Inder, T.E., Warfield, S.K., Wang, H., Huppi, P.S., Volpe, J.J., 2005. Abnormal cerebral structure is present at term in premature infants. Pediatrics 115, 286–294.

Jenkinson, M., Smith, S., 2001. A global optimisation method for robust affine registration of brain images. Med. Image Anal. 5, 143–156.

Jones, D.K., Cercignani, M., 2010. Twenty-five pitfalls in the analysis of diffusion MRI data. NMR Biomed. 23, 803–820.

Jones, D.K., Knosche, T.R., Turner, R., 2013. White matter integrity, fiber count, and other fallacies: the do's and don'ts of diffusion MRI. NeuroImage 73, 239–254.

Kaur, S., Powell, S., He, L., Pierson, C.R., Parikh, N.A., 2014. Reliability and repeatability of quantitative tractography methods for mapping structural white matter connectivity in preterm and term infants at term-equivalent age. PLoS One 9, e85807.

Keihaninejad, S., Ryan, N.S., Malone, I.B., Modat, M., Cash, D., Ridgway, G.R., Zhang, H., Fox, N.C., Ourselin, S., 2012. The importance of group-wise registration in tract based spatial statistics study of neurodegeneration: a simulation study in Alzheimer's disease. PLoS One 7, e45996.

Kelly, C.E., Cheong, J.L., Gabra Fam, L., Leemans, A., Seal, M.L., Doyle, L.W., Anderson, P.J., Spittle, A.J., Thompson, D.K., 2016. Moderate and late preterm infants exhibit widespread brain white matter microstructure alterations at term-equivalent age relative to term-born controls. Brain Imag Behav 10, 41–49.

Keunen, K., Kersbergen, K.J., Groenendaal, F., Isgum, I., de Vries, L.S., Benders, M.J., 2012. Brain tissue volumes in preterm infants: prematurity, perinatal risk factors and neurodevelopmental outcome: a systematic review. J. Matern. Fetal Neonatal Med. 25 (Suppl. 1), 89–100.

Knickmeyer, R.C., Xia, K., Lu, Z., Ahn, M., Jha, S.C., Zou, F., Zhu, H., Styner, M., Gilmore, J.H., 2016. Impact of Demographic and Obstetric Factors on Infant Brain Volumes: A Population Neuroscience Study. Cereb Cortex. https://doi.org/10.1093/cercor/bhw331.

Kuklisova-Murgasova, M., Aljabar, P., Srinivasan, L., Counsell, S.J., Doria, V., Serag, A., Gousias, I.S., Boardman, J.P., Rutherford, M.A., Edwards, A.D., Hajnal, J.V., Rueckert, D., 2011. A dynamic 4D probabilistic atlas of the developing brain. NeuroImage 54, 2750–2763.

Leemans, A., Jones, D.K., 2009. The B-matrix must be rotated when correcting for subject motion in DTI data. Magn. Reson. Med. 61, 1336–1349.

Li, K., Sun, Z., Han, Y., Gao, L., Yuan, L., Zeng, D., 2015. Fractional anisotropy alterations in individuals born preterm: a diffusion tensor imaging meta-analysis. Dev. Med. Child Neurol. 57, 328–338.

Lindstrom, K., Lindblad, F., Hjern, A., 2011. Preterm birth and attention-deficit/hyperactivity disorder in schoolchildren. Pediatrics 127, 858–865.

Lindstrom, K., Winbladh, B., Haglund, B., Hjern, A., 2007. Preterm infants as young adults: a Swedish national cohort study. Pediatrics 120, 70–77.

Manuck, T.A., Rice, M.M., Bailit, J.L., Grobman, W.A., Reddy, U.M., Wapner, R.J., Thorp, J.M., Caritis, S.N., Prasad, M., Tita, A.T., Saade, G.R., Sorokin, Y., Rouse, D.J., Blackwell, S.C., Tolosa, J.E., Eunice Kennedy Shriver National Institute of Child, H., Human Development Maternal-Fetal Medicine Units, N, 2016. Preterm neonatal morbidity and mortality by gestational age: a contemporary cohort. Am J Obstet

Gynecol 215, 103 e101–103 e114.
Mewes, A.U., Huppi, P.S., Als, H., Rybicki, F.J., Inder, T.E., McAnulty, G.B., Mulkern, R.V., Robertson, R.L., Rivkin, M.J., Warfield, S.K., 2006. Regional brain development in serial magnetic resonance imaging of low-risk preterm infants. Pediatrics 118, 23–33.
Moster, D., Lie, R.T., Markestad, T., 2008. Long-term medical and social consequences of preterm birth. N. Engl. J. Med. 359, 262–273.
Munakata, S., Okada, T., Okahashi, A., Yoshikawa, K., Usukura, Y., Makimoto, M., Hosono, S., Takahashi, S., Mugishima, H., Okuhata, Y., 2013. Gray matter volumetric MRI differences late-preterm and term infants. Brain and Development 35, 10–16.
Oishi, K., Mori, S., Donohue, P.K., Ernst, T., Anderson, L., Buchthal, S., Faria, A., Jiang, H.Y., Li, X., Miller, M.I., van Zijl, P.C.M., Chang, L.D., 2011. Multi-contrast human neonatal brain atlas: application to normal neonate development analysis. NeuroImage 56, 8–20.
Padilla, N., Alexandrou, G., Blennow, M., Lagercrantz, H., Aden, U., 2015. Brain growth gains and losses in extremely preterm infants at term. Cereb. Cortex 25, 1897–1905.
Pandit, A.S., Ball, G., Edwards, A.D., Counsell, S.J., 2013. Diffusion magnetic resonance imaging in preterm brain injury. Neuroradiology 55 (Suppl. 2), 65–95.
Pecheva, D., Yushkevich, P., Batalle, D., Hughes, E., Aljabar, P., Wurie, J., Hajnal, J.V., Edwards, A.D., Alexander, D.C., Counsell, S.J., Zhang, H., 2017. A tract-specific approach to assessing white matter in preterm infants. NeuroImage 157, 675–694.
Peterson, B.S., Anderson, A.W., Ehrenkranz, R., Staib, L.H., Tageldin, M., Colson, E., Gore, J.C., Duncan, C.C., Makuch, R., Ment, L.R., 2003. Regional brain volumes and their later neurodevelopmental correlates in term and preterm infants. Pediatrics 111, 939–948.
Pogribna, U., Yu, X., Burson, K., Zhou, Y., Lasky, R.E., Narayana, P.A., Parikh, N.A., 2013. Perinatal clinical antecedents of white matter microstructural abnormalities on diffusion tensor imaging in extremely preterm infants. PLoS One 8, e72974.
Raffelt, D.A., Tournier, J.D., Smith, R.E., Vaughan, D.N., Jackson, G., Ridgway, G.R., Connelly, A., 2017. Investigating white matter fibre density and morphology using fixel-based analysis. NeuroImage 144, 58–73.
Raju, T.N., Higgins, R.D., Stark, A.R., Leveno, K.J., 2006. Optimizing care and outcome for late-preterm (near-term) infants: a summary of the workshop sponsored by the National Institute of Child Health and Human Development. Pediatrics 118, 1207–1214.
Rogers, C.E., Barch, D.M., Sylvester, C.M., Pagliaccio, D., Harms, M.P., Botteron, K.N., Luby, J.L., 2014. Altered gray matter volume and school age anxiety in children born late preterm. J. Pediatr. 165, 928–935.
Rose, S.E., Hatzigeorgiou, X., Strudwick, M.W., Durbridge, G., Davies, P.S., Colditz, P.B., 2008. Altered white matter diffusion anisotropy in normal and preterm infants at term-equivalent age. Magn. Reson. Med. 60, 761–767.
Scarpazza, C., Tognin, S., Frisciata, S., Sartori, G., Mechelli, A., 2015. False positive rates in Voxel-based Morphometry studies of the human brain: should we be worried? Neurosci. Biobehav. Rev. 52, 49–55.
Schwarz, C.G., Reid, R.I., Gunter, J.L., Senjem, M.L., Przybelski, S.A., Zuk, S.M., Whitwell, J.L., Vemuri, P., Josephs, K.A., Kantarci, K., Thompson, P.M., Petersen, R.C., Jack Jr., C.R., Alzheimer's Disease Neuroimaging, I., 2014. Improved DTI registration allows voxel-based analysis that outperforms tract-based spatial statistics. NeuroImage 94, 65–78.
Shah, D.K., Anderson, P.J., Carlin, J.B., Pavlovic, M., Howard, K., Thompson, D.K., Warfield, S.K., Inder, T.E., 2006. Reduction in cerebellar volumes in preterm infants: relationship to white matter injury and neurodevelopment at two years of age. Pediatr. Res. 60, 97–102.
Shapiro-Mendoza, C.K., Lackritz, E.M., 2012. Epidemiology of late and moderate preterm birth. Semin. Fetal Neonatal Med. 17, 120–125.
Smith, S.M., 2002. Fast robust automated brain extraction. Hum. Brain Mapp. 17, 143–155.
Smith, S.M., Jenkinson, M., Johansen-Berg, H., Rueckert, D., Nichols, T.E., MacKay, C.E., Watkins, K.E., Ciccarelli, O., Cader, M.Z., Matthews, P.M., Behrens, T.E., 2006. Tract-based spatial statistics: voxelwise analysis of multi-subject diffusion data. NeuroImage 31, 1487–1505.
Spittle, A.J., Thompson, D.K., Brown, N.C., Treyvaud, K., Cheong, J.L., Lee, K.J., Pace, C.C., Olsen, J., Allinson, L.G., Morgan, A.T., Seal, M., Eeles, A., Judd, F., Doyle, L.W., Anderson, P.J., 2014. Neurobehaviour between birth and 40 weeks' gestation in infants born < 30 weeks' gestation and parental psychological wellbeing: predictors of brain development and child outcomes. BMC Pediatr. 14, 111.
Srinivasan, L., Dutta, R., Counsell, S.J., Allsop, J.M., Boardman, J.P., Rutherford, M.A., Edwards, A.D., 2007. Quantification of deep gray matter in preterm infants at term-equivalent age using manual volumetry of 3-tesla magnetic resonance images. Pediatrics 119, 759–765.
Telford, E.J., Cox, S.R., Fletcher-Watson, S., Anblagan, D., Sparrow, S., Pataky, R., Quigley, A., Semple, S.I., Bastin, M.E., Boardman, J.P., 2017. A latent measure explains substantial variance in white matter microstructure across the newborn human brain. Brain Struct. Funct. 222, 4023–4033.
Teune, M.J., Bakhuizen, S., Gyamfi Bannerman, C., Opmeer, B.C., van Kaam, A.H., van Wassenaer, A.G., Morris, J.M., Mol, B.W., 2011. A systematic review of severe morbidity in infants born late preterm. Am. J. Obstet. Gynecol. 205 (374), e371–e379.
Thompson, D.K., Inder, T.E., Faggian, N., Johnston, L., Warfield, S.K., Anderson, P.J., Doyle, L.W., Egan, G.F., 2011. Characterization of the corpus callosum in very preterm and full-term infants utilizing MRI. NeuroImage 55, 479–490.
Thompson, D.K., Kelly, C.E., Chen, J., Beare, R., Alexander, B., Seal, M.L., Lee, K., Matthews, L.G., Anderson, P.J., Doyle, L.W., Spittle, A.J., Cheong, J.L.Y., 2019. Early life predictors of brain development at term-equivalent age in infants born across the gestational age spectrum. NeuroImage 185, 813–824.
Thompson, D.K., Lee, K.J., Egan, G.F., Warfield, S.K., Doyle, L.W., Anderson, P.J., Inder, T.E., 2014. Regional white matter microstructure in very preterm infants: predictors and 7 year outcomes. Cortex 52, 60–74.
Thompson, D.K., Warfield, S.K., Carlin, J.B., Pavlovic, M., Wang, H.X., Bear, M., Kean, M.J., Doyle, L.W., Egan, G.F., Inder, T.E., 2007. Perinatal risk factors altering regional brain structure in the preterm infant. Brain 130, 667–677.
Thompson, D.K., Wood, S.J., Doyle, L.W., Warfield, S.K., Lodygensky, G.A., Anderson, P.J., Egan, G.F., Inder, T.E., 2008. Neonate hippocampal volumes: Prematurity, perinatal predictors, and 2-year outcome. Ann. Neurol. 63, 642–651.
Tustison, N.J., Avants, B.B., Cook, P.A., Zheng, Y., Egan, A., Yushkevich, P.A., Gee, J.C., 2010. N4ITK: improved N3 bias correction. IEEE Trans. Med. Imaging 29, 1310–1320.
Van Hecke, W., Leemans, A., D'Agostino, E., De Backer, S., Vandervliet, E., Parizel, P.M., Sijbers, J., 2007. Nonrigid coregistration of diffusion tensor images using a viscous fluid model and mutual information. IEEE Trans. Med. Imaging 26, 1598–1612.
Van Hecke, W., Leemans, A., De Backer, S., Jeurissen, B., Parizel, P.M., Sijbers, J., 2010. Comparing isotropic and anisotropic smoothing for voxel-based DTI analyses: a simulation study. Hum. Brain Mapp. 31, 98–114.
Veraart, J., Sijbers, J., Sunaert, S., Leemans, A., Jeurissen, B., 2013. Weighted linear least squares estimation of diffusion MRI parameters: strengths, limitations, and pitfalls. NeuroImage 81, 335–346.
Walsh, J.M., Doyle, L.W., Anderson, P.J., Lee, K.J., Cheong, J.L., 2014. Moderate and late preterm birth: effect on brain size and maturation at term-equivalent age. Radiology 273, 232–240.
Winkler, A.M., Webster, M.A., Brooks, J.C., Tracey, I., Smith, S.M., Nichols, T.E., 2016. Non-parametric combination and related permutation tests for neuroimaging. Hum. Brain Mapp. 37, 1486–1511.
Yaari, M., Mankuta, D., Harel-Gadassi, A., Friedlander, E., Bar-Oz, B., Eventov-Friedman, S., Maniv, N., Zucker, D., Yirmiya, N., 2018. Early developmental trajectories of preterm infants. Res. Dev. Disabil. 81, 12–23.
Zhang, H., Schneider, T., Wheeler-Kingshott, C.A., Alexander, D.C., 2012. NODDI: practical in vivo neurite orientation dispersion and density imaging of the human brain. NeuroImage 61, 1000–1016.